

# Dual flow fusion model for concrete surface crack segmentation

Yuwei Duan, Xun Lin, Wenzhong Tang, Xiaolei Qu

Corresponding author(s). E-mail(s): zy2006211@buaa.edu.cn

**Abstract** Cracks and other diseases are important factors that threaten the safe operation of transportation infrastructure. Traditional manual detection and ultrasonic instrument detection consume a lot of time and resource costs. With the development of deep learning technology, many deep learning models are widely used in actual visual segmentation tasks. The detection method based on the deep learning model has the advantages of high detection accuracy, fast detection speed and simple operation. However, the crack segmentation based on deep learning has problems such as sensitivity to background noise, rough edges, and lack of robustness. Therefore, this paper proposes a fissure segmentation model based on two-stream fusion, which simultaneously inputs images into two designed processing streams to independently extract long-distance dependent and local detail features, and realizes adaptive prediction through a dual-head mechanism. At the same time, a new interactive fusion mechanism is proposed to guide the complementarity of different levels of features to realize the location and identification of cracks in complex backgrounds. Finally, we propose an edge optimization method to improve segmentation accuracy. Experiments have proved that the F1 value of the segmentation results on the DeepCrack[1] public dataset reached 93.7%, and the IOU value reached 86.6%; the F1 value of the segmentation results on the CRACK500[2] dataset reached 78.1%, and the IOU value reached 66.0%.

**Index Terms:** transformer, crack segmentation, feature interaction

## I. INTRODUCTION

Railway transportation is the main artery of our country's national economy. With the increase of operation time, affected by climate, environment and service time, cracks and other deterioration phenomena gradually appear on the surface of bridge concrete, which brings hidden trouble to the safe operation. Bridge cracks for the safety of the bridge has a great harm: accelerate concrete carbonization, reduce the corrosion resistance of concrete to various corrosive media, affect the structural strength and stability of concrete structures. Therefore, it

is very necessary to research on intelligent detection system and key technologies of superficial cracking of concrete and steel structure in high-speed rail infrastructure. The development process of crack detection technology is mainly divided into traditional image processing, traditional machine learning method and deep learning method. The traditional image processing method has high requirements on image preprocessing technology, and the detection results are easily affected by lighting, noise and other factors. The detection method based on machine learning was adopted morphological detection method in the early stage. In the later stage, seed points, tensor voting and other methods are adopted, which makes the calculation complicated and the model inefficient, unable to cope with complex scenes.

Deep learning crack detection methods are usually based on convolutional neural networks. Convolutional neural network also achieves good results in multiple visual tasks due to its nonlinearity and rotation invariance. The convolutional model utilizes continuous convolution operation on the image to obtain the features of the image. However, it has the following limitations: insufficient receptive field and loss of detail information during downsampling. Although existing studies have proposed a variety of ways to expand CNN receptive field, such as FPN[3] and ASPP[4]. The former uses feature pyramid to enlarge receptive field layer by layer, while the latter uses void convolution to enlarge receptive field, these ways cannot effectively solve the problem of lack of global features. In the crack segmentation task, the global feature provides the location of the crack region, ensures the topological integrity, and helps the model recognize different texture features in the complex background. In order to solve the problem of lack of global features, the Vision Transformer[5] model based on multi-head self-attention calculation encodes the image into multiple patches and calculates self-attention between patches to extract long distance dependencies. However, the calculation amount of this calculation method is much larger than that of convolutional neural network, and the relationship between pixels inside patch is ignored. Such detailed information is very important for crack edge perception, and is an indispensable element in intensive prediction.

In order to take into account global information and local information and improve segmentation accuracy, some methods propose combining CNN and Transformer to solve the problem. CvT[6] converts linear projection in self-attention block into convolutional projection. The GLTB module in EHT uses numerical addition to numerically add local features to global

features. The Conformer model relies on feature coupling units (FCU) to interactively fuse local feature representations and global feature representations at different resolutions. DS-Net[7] proposes a two-flow framework that fuses convolution and self-attention through cross attention, in which the scale of each form learns to align with the others. However, convolution and attention have inherently conflicting properties, which can lead to ambiguity in training.

In this paper, a parallel two-stream architecture is used to extract image features. The two-stream parallel architecture ensures the independence and integrity of feature extraction. At the same time, in the use of features, but only feature extraction is not enough, in order to make global features and local features mutually auxiliary: global features through multi-head attention to obtain different levels of probability graph, guide the model to focus on the parts that may be interested. Under the guidance of global features, local features can eliminate noise interference and provide details between pixels, such as capturing abrupt changes between pixels so as to accurately identify edges. Some existing fusion methods, for example, some models adopt superposition in channel dimension to enrich features, and the models can adapt to learn features at different levels. Although the above fusion method has achieved some results, it neglects the effective communication between the features. Therefore, we propose a two-stream feature extraction module, and insert the feature interaction process in the middle of two parallel streams. Through multi-scale feature fusion, the semantic features are further enriched. The contributions of this paper are as follows:

1. Using the dual-flow structure, the CNN and Transformer branches can respectively preserve the local features and global representation to the maximum extent.
2. Interaction modules that employ both global and local features derive from adaptive fusion features.
3. The best segmentation results are experimentally verified on multiple public data sets.

## **II. RELATED WORKS**

With the continuous development of deep learning, compared with traditional digital image processing methods, deep learning has advantages such as high detection accuracy and good robustness. There are several typical researches on concrete superficial crack detection based on image segmentation: convolution based segmentation model, Transformer based segmentation model, combined with convolution and Transformer segmentation.

**Segmentation based on convolution.** Traditional convolution utilizes an aggregation function on the local receptive field according to the weights of the convolution, which are shared throughout the feature graph. Inherent features introduce a crucial inductive bias to image processing. Due to the small pixel proportion and small width of the crack itself, which is very similar to the edge segmentation of the image, DeepCrack method conducts crack segmentation based on the HED[8] edge segmentation network. The DeepCrack model samples the results of each downsampling to the size of the original image through the by-pass tributary, and then conducts loss calculation through deep supervision. To further improve the accuracy of the edge. Wang Sen et al. adopted full convolutional neural network to detect cracks in images, and constructed Crack FCN[9], which is more suitable for crack detection. Since there are few pixels in the Crack image, Crack FCN cancels the Dropout function on the basis of FCN to reduce local information loss, and uses a higher-scale deconvolution layer to expand local details while deepening the network depth of FCN. The experimental results show that this Crack FCN has stronger fine discrimination ability, higher detection accuracy and lower false detection rate for cracks. Wang et al. proposed a new improved model based on the original Deeplabv2[10] to adapt to the particularity of crack damage detection. Compared with previous methods, this method can yield very high precision output, and a new method for marking cracks is proposed, which is conducive to the measurement of crack length and width. Yang Min constructed the SPPNet[11] network for the problem of tunnel crack detection. Using the ideas of Deeplab and PSPNet[12] to solve this problem, SPPNet integrates multi-scale features of different layers, so that there is a lot of information at the upper level of the network in the final upsampled feature map.

Segmentation based on Transformer. The Self-Attention module uses a weighted average operation based on the context of input features to dynamically calculate the weight of attention through the similarity function between the relevant pixel pairs. This flexibility allows the attention module to focus on different areas adaptively and capture more features. The ViT model splits the image into multiple patches and maps them into a linear embedded sequence, encoded with encoders, and establishes long-distance dependent features by calculating global correlation through multi-head self-attention mechanisms. In the STER[13] model, after the image is encoded, features of different scales are extracted through downsampling of 4

Transformer blocks, then features of different scales are up-sampled to the resolution of the original image, and targets of different scales are captured by superimposing 4 feature maps on channel dimensions. Segmentor[14], as a pure Transformer coding-decoding architecture, takes advantage of the global image context of each layer of the model. On the original ViT model, Mask Transformer is proposed to decode the output embedded by encoders and classes in the decoding stage, and Argmax is applied to classify each pixel one by one after upsampling, and the final pixel segmentation map is output. It further improves the poor performance of ViT in small training sets.

**Feature fusion.** Given the different and complementary nature of convolution and Self-Attention, there is the potential to benefit from both paradigms by integrating these modules. U-Net[15] superposes features at different levels by jumping joins, and FPN utilizes a propagation path from the top down to connect multi-scale features. ASPP in DeepLabv3[16] set up cavity convolution with different expansion coefficients to obtain different scale features. In view of the limitation of the receptive field of convolutional neural networks, many studies consider the fusion of global and local features. SegFormer[17] uses a Lightweight All-MLP Decoder to aggregate information from different layers to combine local and global attention for a powerful representation. DS-Net computes fine-grained and integrated features simultaneously, proposes an intra-scale propagation module to handle two different resolutions in each block, and proposes an inter-scale alignment module to perform cross-feature information interaction on a dual scale. Conformer[18] relies on feature coupling unit (FCU) to input local feature and global feature into two parallel concurrent feature processing streams respectively to complete feature interaction. This paper focuses on effective interaction of global features with local features, avoiding interference from invalid information.

### III. METHOD

The proposed model (CrackFuse) is shown in Figure 1 below: dual-flow based architecture: Feature extraction is carried out concurrently by Transformer global processing flow and convolutional local processing flow, while feature interaction and multi-level fusion are achieved through BiFuse Module interaction module.

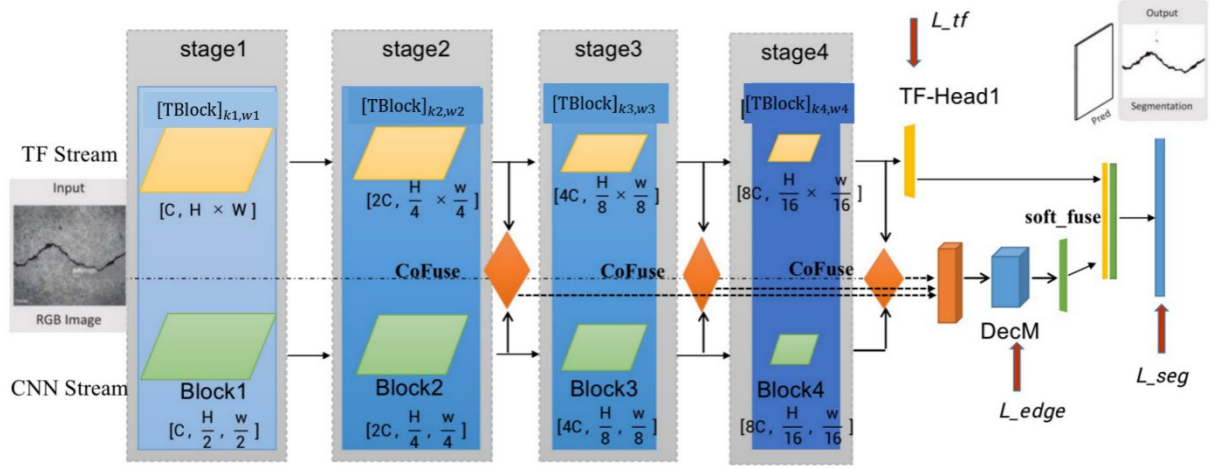


Figure 1 Overall structure diagram of the model

### 3.1 Dual-scale Representations

CNN collects local features stratified by a convolution operation and preserves local cues as features. Vision Transformer is thought to aggregate the global representation in a soft way between compressed patch embedding via a cascading Self-Attention module. By processing images concurrently, the multi-layered features of the image can be preserved to the maximum extent.  $x$  for a given image, the size of  $W \times H \times 3$ , DSM is defined as D dual flow network image  $x$  after input to D, M get test result. Define  $x_i$  the pixels in the image,  $D(x_i)$  based on dual flow network said the prediction results of each pixel,  $D(x_i) \in \{0, 1\}$ . A collection of all the predictions of a pixel is dual flow network D for image  $x$  crack damage area segmentation results, as shown in formula 1. See the detailed structure of each module of Network D below.

$$M \leftarrow \{D(x_i)\}, \quad i = 1, 2, \dots, W \times H \quad (1)$$

**Global representation** adopts the Cswin Transformer[19] model with a small number of parameters. The image is divided into multiple patches, and each patch is encoded and input into the following four blocks to calculate the long-distance dependence. In the method of cross attention, each patch only pays attention to the cross window which is located in the same row as it. In the top-down calculation, the attention window expands layer by layer, and finally the features of the whole image are aggregated. Referring to the structure of feature pyramid, multi-level features can be aggregated in a better way. After the features of all layers are interpolated and upsampled to the same dimension, the final global features of 4\*channel can be generated by jumping and joining. The overall formula of global branches is as follows: Formula 2 and Formula 3.

$$X_g^i = \text{Transformer}_{\text{Block}_i}(X_g^{i-1}) \quad (2)$$

$$X_g = F(\text{Upsample}(X_g^1 | X_g^2 | X_g^3 | X_g^4)) \quad (3)$$

The four-stage process of global processing branch is shown in Figure 2. The input of the first stage is the image block coding vector, the number of channels is  $C$ , and  $\frac{H}{4} \times \frac{W}{4}$  is the total dimension of the vector. Convolution operation is used in each adjacent stage to reduce the feature scale and increase the number of channels. After the feature processing of stage  $i$ , the output feature graph size is  $\frac{H}{2^{i+1}} \times \frac{W}{2^{i+1}} \times 2^i C$ . Each  $\text{stage}_i$  consists of  $N_i$  modules  $\text{TBlock}_i$ , where  $N_i$  is the parameter of the model.

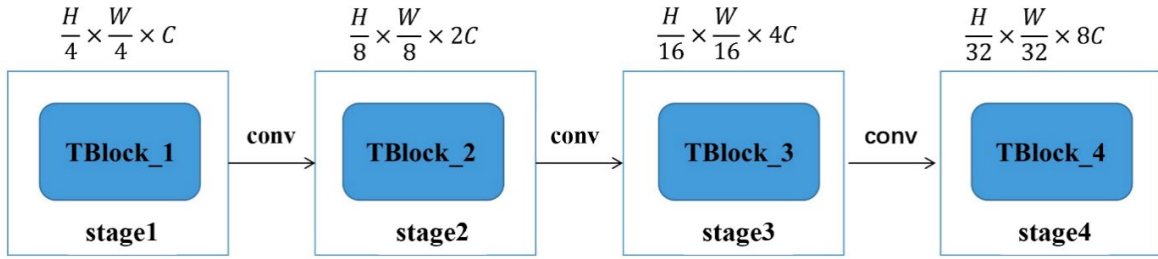


Figure 2 Four-stage processing of CSwin Transformer

The TBlock consists of the multi-head self-attention computing module Cross MSA and the forward propagation FFM module, with jump connections added to prevent the gradient from disappearing. Formula 4 and 5 are calculated as follows:

$$X_l = \text{Attention}(\text{LN}(X_{l-1})) + X_{l-1} \quad (4)$$

$$\tilde{X}_l = \text{MLP}(\text{LN}(X_l)) + X_l \quad (5)$$

Where represents the output of the input TBlock module and is the output of the input TBlock module.  $X_{l-1}$  represents the layer normalization processing, and MLP is the multilayer perceptron.

**Local representation** is to obtain more shallow information, such as details of edges and contours. Drawing on the edge detection model HED and based on the FPN network model, a bottom-up and top-down processing flow is designed. In the middle of the two reverse processing flows, phased features are fused to obtain more accurate features.

In the local processing branch, as shown in Figure 3 below, the fourth stage outputs the feature vector with the size of  $B \times 512 \times 24 \times 24$ . After three times of double upsampling, the feature scale gradually recovers to, and, where  $B$  is the number of images trained in each batch of the model.  $B \times 256 \times 48 \times 48$ ,  $B \times 128 \times 96 \times 96$ ,  $B \times 64 \times 192 \times 192$ . The result of down-sampling at each stage in the local processing branch is called, representing the first stage.

$F_{l\_down}^i$ , by the same token, the upsampled result is called  $F_{l\_up}^i$ . Finally, the sum of the same stage is taken as the output of the local processing stream.  $F_{l\_down}^i, F_{l\_up}^i$  Formula 6 is as follows:

$$F_l^i = f\left(F_{l\_down}^i \mid F_{l\_up}^i\right), \quad i = 2, 3, 4 \quad (6)$$

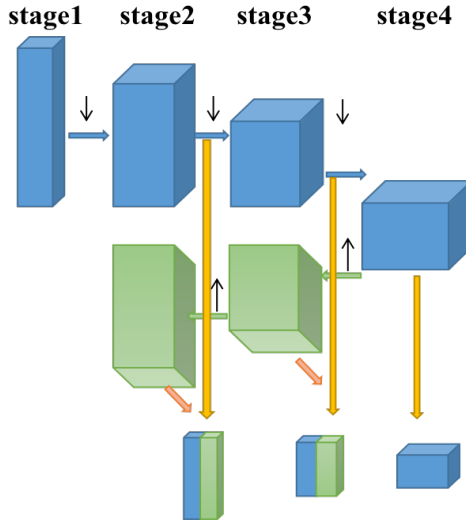
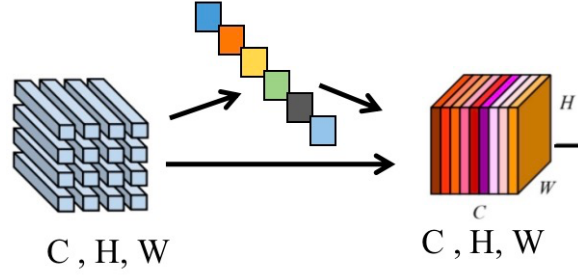


Figure 3 Local processing branch structure diagram

### 3.2 Fuse interaction Module

**Feature Alignment** inserts parallel fusion modules in the middle of two processing streams for feature interactive fusion. The input of the module is the intermediate feature of the output of each stage in the global processing flow and the local processing flow, achieving the effect of simultaneous extraction and fusion. The features output by the global processing stream first need to be reshaped into the same dimension as the local processing stream by a feature alignment operation.

**Feature Refine** further refines and filters the input features in order to retain valid information and avoid interference from invalid information in the fusion process. Channel Attention draws on SENet's[20] ideas, and can correct the features of channels by re-modeling the relationship between channels through squeeze and extend operations, so as to improve the characterization ability of neural networks. Global information can be used to strengthen useful features and dilute useless ones. squeeze first to compress the features of each channel as the descriptor for that channel, by means of mean pooling, averaging the features within the channel.



**Figure 4 Schematic diagram of channel attention calculation**

The specific operation formula (7-9) is as follows:

$$Z_c = f_{sq}(F_g) = avg(F_g) = \frac{1}{H \times W} \sum_{i=1}^H \sum_{j=1}^W F(i, j) \quad (7)$$

$$S = f_{ex}(\{Z_c | W\}) = \sigma(g(Z, W)) = \sigma(W_2 \cdot \delta(W_1 \cdot Z)) \quad (8)$$

$$\tilde{F}_g = f(F_g, S) = F_g \cdot S \quad (9)$$

S is the vector of C dimension, is the weight of the learned channel, useless features will be tended to 0. Activate the function and  $\delta$ ,  $\sigma$  are selected as ReLU and sigmoid in turn. W is the set of weight  $W_1$  and  $W_2$  matrices, including Where the dimension is  $\mathbb{R}^{\frac{C}{r} \times C}$  and  $\mathbb{R}^{C \times \frac{C}{r}}$ .

**Spatial Attention** Local features contain a lot of low-level details, but not all the low-level information is useful, background texture, lighting and other factors will often interfere with the model. We believe that channel attention can tell the model which features are meaningful, so we use spatial attention in local features to further remove these redundant noises.

$$M_s(F_l^i) = \sigma(f^{7 \times 7}([AvgPool(F_l^i), MaxPool(F_l^i)])) \quad (10)$$

Input is feature F of  $R^{H \times W \times C}$  is the local feature. First, maximum pooling and average pooling of channel dimensions are carried out to obtain two  $H \times W \times 1$  channel descriptions, and the two descriptions are splicing together according to channels. Then, after the Compress operation and sigmoid function activation, the weight coefficient is obtained.  $M_s^i$  Multiply the input feature F to get the scaled new feature.

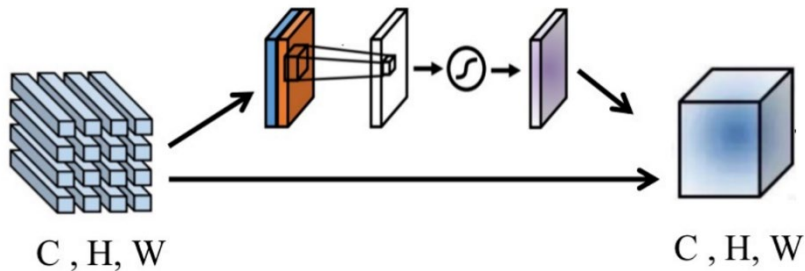


**Figure 5 Schematic diagram of spatial attention calculation**

$$F_l^i = F_{scale}(F_l^i, M_s^i) = F_l^i \cdot M_s^i \quad (11)$$

**Feature Interaction** firstly consists of global features  $X_g^i$  and local features  $F_l^i$  super imposed on the channel dimension. Then, combined features  $F_{cat}$  are input into CoFusion module for feature interaction and correlation calculation. It consists of a three-layer MLP. Use the softmax function in front of the output of the MLP to generate adaptive weights for different channels. Finally, the obtained correlation probability graph is applied to the original feature graph to complete the feature interaction.

$$CorrMap^i = \partial \left( b_2 + W_2 \left( b_1 + W_1 \left( [F_l^i, X_g^i] \right) \right) \right) \quad (12)$$

$$F_{fuse}^i = CorrMap^i \times [F_l^i, X_g^i] \quad (13)$$

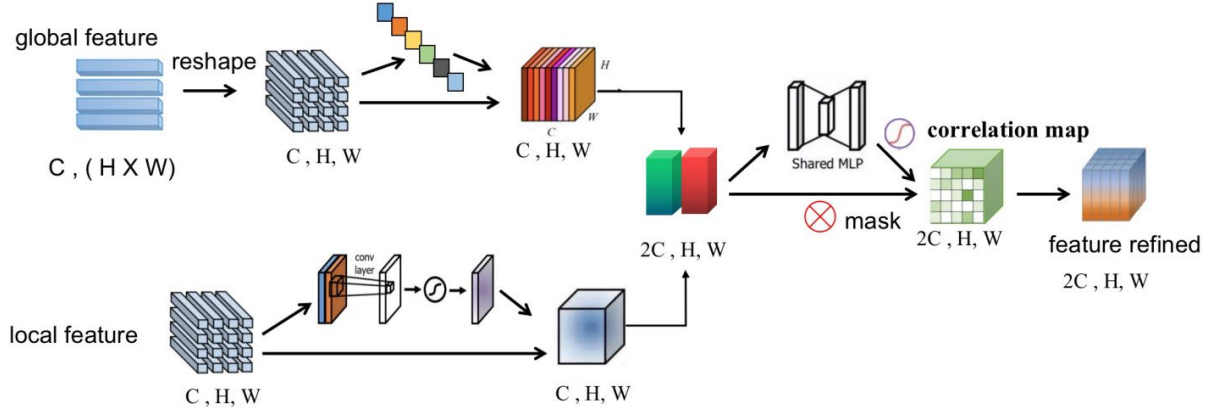


**Figure 6 Detailed structure diagram of feature fusion module**

### 3.3 Decouple Module

In order to extract the edge information to the crack damage accurately, design the edge optimization module. The main part of the feature is decoupled from the contour part, and the edge supervision is added to optimize the feature extraction of the edge part. We use continuous down sampling to obtain the pseudo-clustering center, and then the original feature is projected to correct according to the pseudo-clustering center. The edge information  $F_{edge}$  can be obtained by subtracting the main feature from the original feature.

$$F_{flow} = \gamma \left( \left[ Up \left( Down(F_{fuse}) \right), F_{fuse} \right] \right) \quad (14)$$

$$F_{body} = Grid_{sample}(F_{fuse}, Grid^{h \times w} + F_{flow}) \quad (15)$$

$$F_{edge} = cat(F_{fuse} - F_{seg\_wrap}, F_{fuse}^1) \quad (16)$$

$$F_{final} = F_{edge} + F_{body} \quad (17)$$

### 3.4 Objective Function.

The losses adopted in this paper are divided into structural loss and edge loss. The structural

loss is used to supervise the final prediction accuracy of the Function, and the edge loss is used to supervise the accuracy of edge extraction. The overall loss is composed of the following parts:

$$L_{all} = \theta_0 L_{final} + \theta_1 L_{global} + \theta_2 L_{local} + \theta_3 L_{edge} \quad (18)$$

Where  $\theta_0, \theta_1, \theta_2, \theta_3$  is the weight parameter, which is used to weigh the proportion of different losses.

Where  $L_{final}, L_{global}, L_{local}$  is used to calculate the loss of the overall structure of the image. The overall loss is divided into two parts, including pixel level binary cross entropy loss and intersection ratio loss. Where  $P$  is the total number of all pixels,  $i$  is a certain pixel, and the true pixel value  $y_i$ ,  $P(x_i)$  is the predicted probability.

$$L_{BCE} = - \left( \sum_i^p y_i (\log P(x_i) + (1 - y_i) \log P(1 - x_i)) \right) \quad (18)$$

$$L_{IOU} = \frac{\sum_i^p y_i P(x_i)}{\sum_i^p y_i + \sum_i^p P(x_i)} \quad (19)$$

In order to balance the large gap between the ratio of positive and negative pixels and weaken the influence of pixels that are difficult to identify to ensure the accuracy of the overall effect, the weight with weight  $\omega$  is introduced as the loss weight.

$$L_{final} = \omega (L_{BCE} + L_{IOU}) \quad (20)$$

The calculation of edge loss  $L_{edge}$  needs to take into account the extremely unbalanced ratio of positive and negative pixels in a single image: often the edge pixels only occupy a small proportion. Therefore, based on the binary cross entropy at the pixel level, we introduce the adaptive weight mask as the pixel coefficient to calculate the edge loss.

$$L_{edge} = - \left( \frac{\sum(y_i = 0)}{N} \sum_i^p y_i \left( \log P(x_i) + \frac{\sum(y_i = 1)}{N} (1 - y_i) \log P(1 - x_i) \right) \right) \quad (21)$$

#### IV. EXPERIMENTS

**Dataset.** This work makes use of four datasets, CrackForest[21], DeepCrack, CRACK500, CrackTree260[22].

- The CrackForest dataset(CFD) consists of a total of 118 images of size 480×320 pixels. The images have been taken from road surfaces in Beijing. This dataset is then split into 71 training, and 46 testing images.
- CrackTree260 (CT260) is a dataset containing 260 grayscale road pavement images of different sizes (800 × 600 and 960 × 720 pixels).
- A total of 537 RGB images are contained in Deepcrack. The dataset split is given as 300

training, and 237 testing images, all of size  $544 \times 384$  pixels.

- CRACK500 is a dataset containing 3000 RGB images of size  $800 \times 600$  pixels. This dataset is then split into 1500 training, 200 validation and 1300 testing images.

**Evaluation Metrics.** We use F1 score, IOU, Acc to measure the quality of the generated images at pixel level.

**Implementation Details.** We use Adam optimizer with  $\{\beta_1 = 0.5, \beta_2 = 0.999\}$  and train the model for 30 epochs. The learning rate is set to  $1e-4$ , and the batch size is 2.

### **Qualitative Results.**

**Comparison with SOTAs.** We further conduct a comparison experiment with most related SOTA methods on the DeepCrack dataset. A total of six common concrete superficial crack segmentation methods and the classic semantic segmentation network model are selected. The following is the introduction of these models.

- **U-Net** classical semantic segmentation model, U-Net model for encoder-decoder structure, it as a general network model, in the semantic segmentation of various tasks are very good performance.
- **DeepLabv3+** uses the Xception module for task splitting and deep separable convolution into void convolution and decoder modules to achieve high accuracy in the model.
- **R2UNet [23]** introduces residual blocks as well as loop structures on the basis of U-Net;
- **DeepCrack** model is based on edge detection network HED, and a bypass branch is designed to enhance the edge information extracted from shallow network.
- **STRNet[24]** model proposes a new high performance network of depth encoder and attention decoder, which uses channel attention to enhance features during feature extraction, and Transformer is used to build the decoder, adding separable convolution operations in order to achieve real-time detection rate. A semantically trainable representation network is proposed to improve.
- **CrackFormer[25]** model uses attention mechanism to improve the model's crack detection in complex scenes, and proposes a novel attention mode Self AB. The encoder decoder structure based on Transformer integrates Self AB module and Scale AB module. Where Self AB is embedded into different levels of encoder and decoder modules and Scale

AB introduces corresponding decoder between encoder feature map and encoder feature map.

The comparison model is selected based on two principles: first, the source code is disclosed and the code is reproducible; second, the paper will claim that the model has achieved the experimental effect of SOTA. Quantitative experiment and qualitative experiment were carried out respectively in the comparative experiment. Quantitative experiment refers to the numerical comparison of F1 and IOU on the public data set, as shown in the table below. Qualitative experiment refers to the visualization results of crack damage segmentation on superficial concrete images, as shown in the figure. All experimental results are reproduced in the software environment required in the original paper, and the software used is Nvidia 3080 graphics card, and the parameters used in the model are consistent. In this section, the CRACK500 and DeepCrack datasets were selected as the datasets for the crack segmentation task. This is because these two data sets contain the largest number of images, and the images involve rich scenes, which can detect the accuracy of model segmentation and its generalization performance at the same time.

**Table 1 Comparison table of experimental results between Dec\_DSFM model and existing model**

Model	F1 Score		IOU Score	
	CRACK500	DeepCrack	CRACK500	DeepCrack
U-Net	69.4%	90.6%	58.0%	83.2%
DeepLabv3+	67.3%	89.5%	55.9%	81.5%
R2UNet	45.1%	86.7%	34.1%	77.4%
DeepCrack	64.8%	90.5%	58.3%	82.7%
STRNet	65.6%	88.1%	54.8%	79.3%
CrackFormer	69.8%	89.9%	58.6%	82.1%
<b>Dec-DSFM</b>	<b>78.1%</b>	<b>93.7%</b>	<b>66.0%</b>	<b>86.6%</b>

The optimal results in the table are shown in bold. As can be seen from the data in the table, the segmentation accuracy of Dec DSFM model is the highest, and the segmentation results on the two public data sets are 6.0% and 6.0% higher than the average F1 value and the average IOU value of the CrackFormer model with the best performance at present. Images in the CRACK500 dataset contain a variety of cracks: linear, crossed and reticulated. The background texture of the image is complex, in which the contrast between the crack area and the background area is low, which makes the crack segmentation more difficult. The Dec-DSFM

model has shown satisfactory results on this dataset, proving its versatility and strong generalization ability for complex scenes. It solves the problem that only a single scene fracture can be detected in some models. The number of images in DeepCrack data set is small, and the width of crack loss area is generally larger than that in CRACK500. It can be seen from the data in the table that the image segmentation accuracy on DeepCrack data set is higher. Among the existing models, U-Net model has a better effect on small data sets. The DeepCrack model adds edge extraction tributaries to further strengthen the accuracy of segmentation results through deep supervision. CrackFormer added Transformer layer to extract long distance dependencies, but the detection effect on small data sets is not good, because of its attention computing is fully connected structure, Transformer on some features of the language, such as sequential, syntax, etc., has no prior inductive bias, and Transformer often needs a lot of data input to learn inductive bias. On the basis of convolutional neural network, STRNet adds compression and expansion operations to correct the weight between channels, further strengthening the characterization of model features. However, the STRNet model does not perform well on the CRACK500 dataset due to the lack of long distance dependencies, thus demonstrating the powerful feature extraction capability of the Dec-DSFM model. Therefore, through comprehensive comparison with the six SOTA methods, the Dec-DSFM model proposed in this paper achieves the optimal effect on the two indexes of the two public data sets, and has remarkable generalization ability, advancement and superiority.

The following figure shows the segmentation results of a comparison experiment between six crack detection models and the model proposed in this paper. The first row is the original image to be detected, the second row is the annotation of the image, the third row is the segmentation results of the model proposed in this paper, the fourth to ninth rows are the segmentation results of the other six models, and the optimal segmentation results are marked with red dotted lines. It can be seen from the display results that the accuracy of the model segmentation is higher than that of other models. U-Net model and DeepLabv3+ model cannot identify fine crack damage, and R2UNet model is easy to be disturbed by noise, resulting in some noise islands on the segmentation results. DeepCrack model has poor segmentation results for slender cracks, and the lack of long-distance dependence leads to disconnection of long-distance cracks. Both STRNet and CrackFormer models are attention-computing models.

STRNet model focuses on ensuring real-time detection rate but cannot take into account the accuracy of segmentation. As a result, the model is prone to interference from some local redundant information, such as contrast, etc. The CrackFormer model cannot accurately identify slender cracks, because the model is completely based on Transformer construction, which fully extracts the high-level semantic information while ignoring the low-level semantic information. Figure 76 shows the segmentation results F1 value and IOU value on the verification set of the above 7 crack segmentation models in the training process as the number of training iterations changes, and the results with the highest accuracy are marked with red lines. As can be seen from the figure, the model proposed in this paper has been performing well in the training process, and all evaluation indexes are higher than other crack loss segmentation models. With the increase of the number of training iterations, the features learned by Dec-DSFM are gradually saturated, and the segmentation accuracy of the model is maintained at a high level.

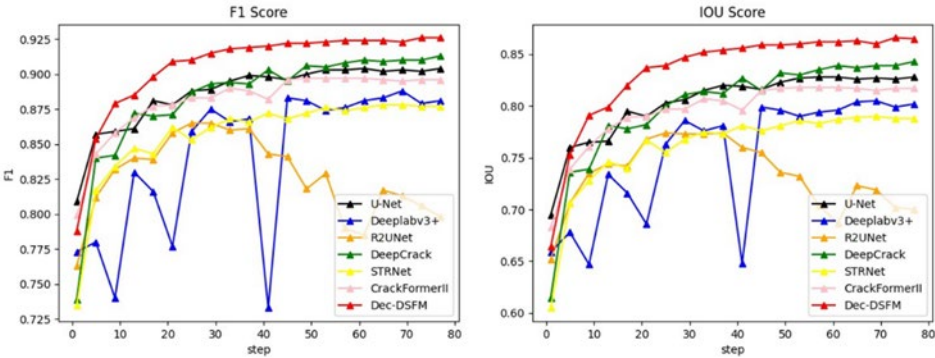


Figure 7 Experimental results of Dec-DSFM and SOTA model

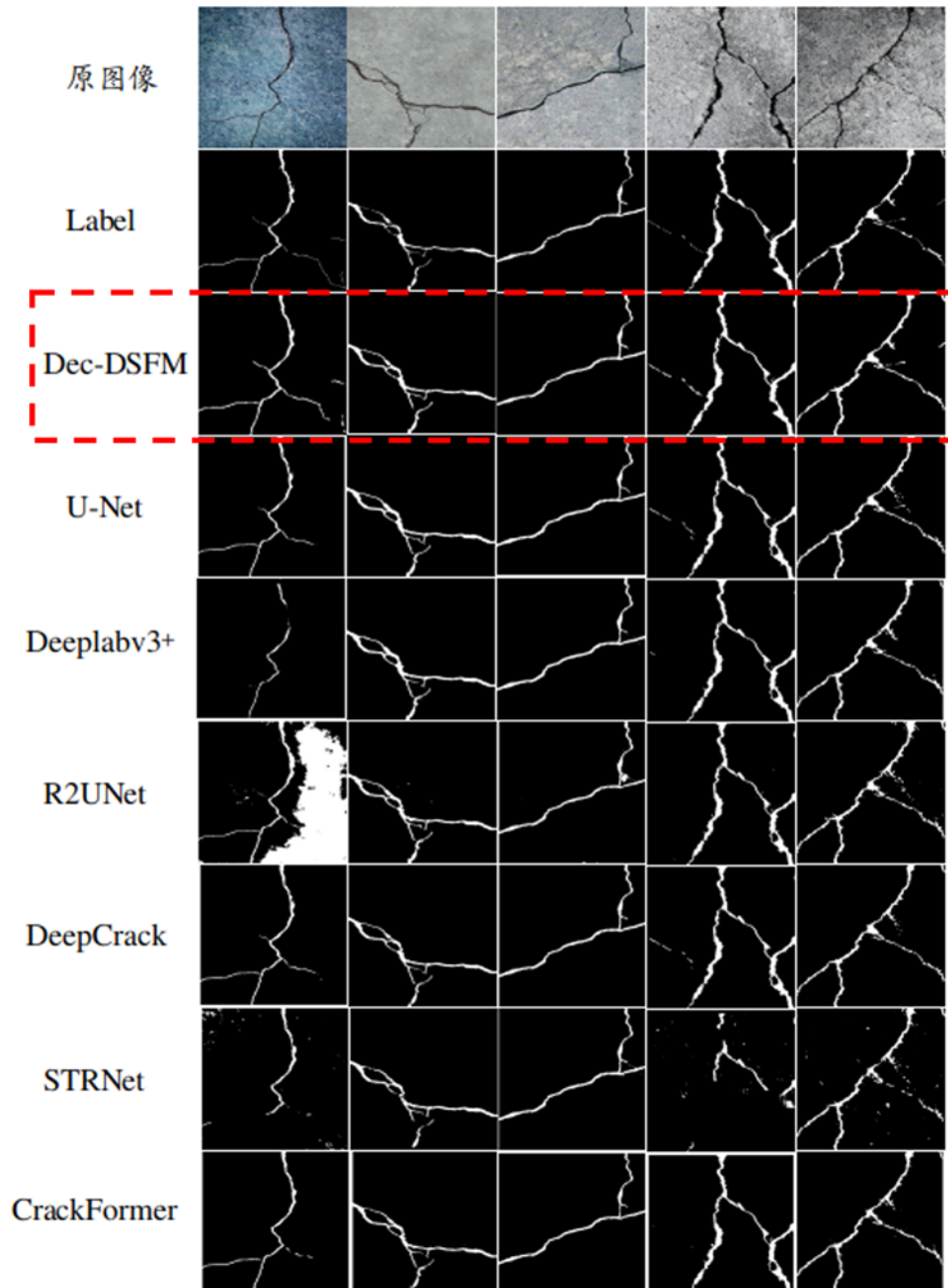


Figure 8 Segmentation results of Dec-DSFM and the existing model

**Ablation experiments** were performed on the CRACK500 data set and on the DeepCrack data set, verifying the effect of the two-flow structure and the characteristic interaction module, respectively. The experimental results are graphically shown in the table 2. It can be seen that the design structure of Transformer and convolutional neural network in dual-flow network can effectively improve the accuracy of the model. After the addition of feature interaction module, the anti-noise ability and the effective extraction of detail information are further improved. Based on the fusion features, the edge optimization strategy is added to further improve the

accuracy of the model for the segmentation of cracked edges.

**Table 2** Ablation results table

模型/策略	F1值		IOU值	
	DeepCrack	CrackForest	DeepCrack	CrackForest
<b>DSM</b>	91.0%	65.8%	83.9%	49.6%
<b>DSM + CoFuse</b>	92.7% (↑1.6%)	68.8% (↑2.8%)	86.5% (↑2.6%)	52.8% (↑3.2%)
<b>DSM + CoFuse + DecM</b>	93.7% (↑1.0%)	69.3% (↑0.5%)	88.3% (↑1.8%)	53.7% (↑0.9%)

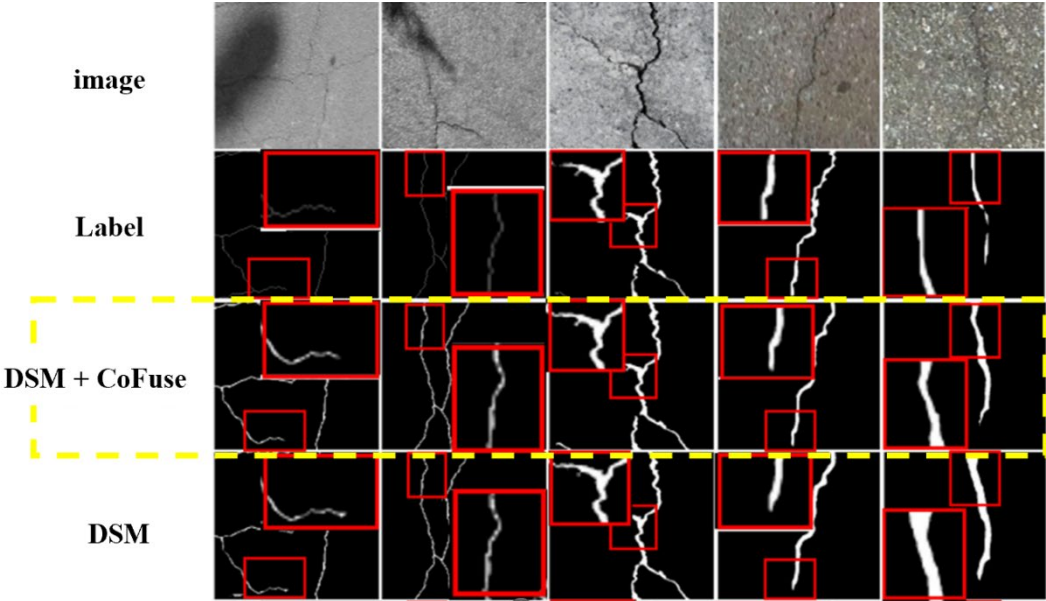


**Figure 9.** Experimental results of CoFuse module ablation

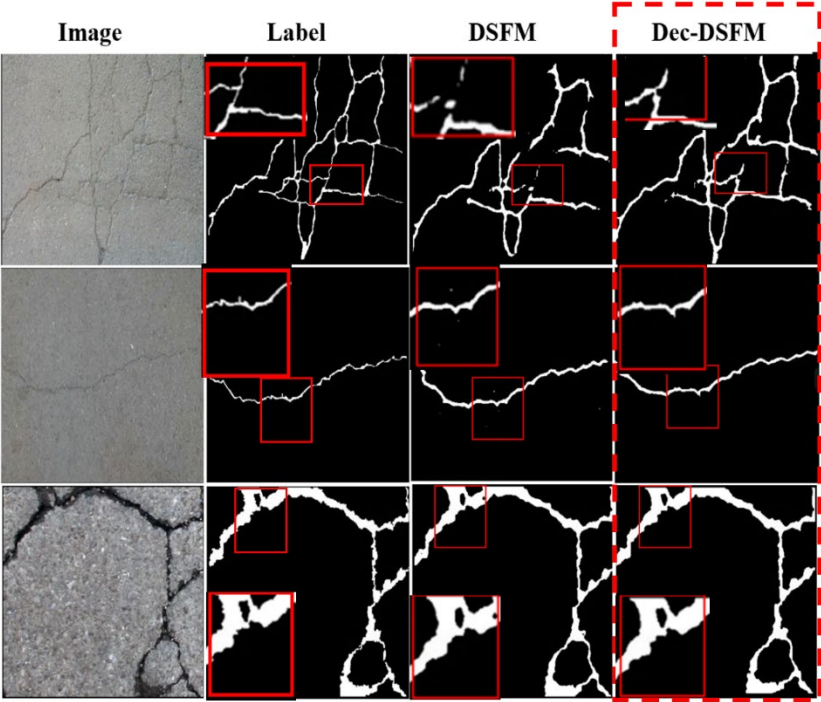


**FIG. 10 Ablation results of DecM**

## **V. CONCLUSION**

In this paper, dual-flow architecture design is adopted, and Transformer model is proposed to obtain the long-distance dependence relationship on the image, which improves the generalization performance of the model and makes our model have better detection effect in the complex background of the real scene. On this basis, in order to make the global features and local features of the model can better interact, we put forward the feature fusion module, in the process of feature extraction feature interaction, so as to better use of the global and local features. In the end, the decoupling method is used to separate the main part and the edge part of the image, which effectively improves the segmentation accuracy of the cracked edge part. In future studies, we will further optimize the extraction of edge parts, lightweight network model, and adapt to multi-scene crack detection and other defect detection.

## **Reference**

- [1] Liu Y, Yao J, Lu X, et al. DeepCrack: A deep hierarchical feature learning architecture for crack segmentation[J]. *Neurocomputing*, 2019, 338: 139-153.
- [2] Zhang L, Yang F, Zhang Y D, et al. Road crack detection using deep convolutional neural network[C]//2016 IEEE international conference on image processing (ICIP). IEEE, 2016: 3708-3712.
- [3] Lin T Y, Dollar P, Girshick R, et al. Feature Pyramid Networks for Object Detection[J]. IEEE Computer Society, 2017.
- [4] Chen L C, Papandreou G, Kokkinos I, et al. Semantic Image Segmentation with Deep Convolutional Nets and Fully Connected CRFs[J]. *Computer Science*, 2014(4):357-361.
- [5] Dosovitskiy A, Beyer L, Kolesnikov A, et al. An image is worth 16x16 words: Transformers for image recognition at scale[J]. *arXiv preprint arXiv:2010.11929*, 2020.
- [6] Wu H, Xiao B, Codella N, et al. CvT: Introducing Convolutions to Vision Transformers[J]. 2021.
- [7] Mao M, Zhang R, Zheng H, et al. Dual-stream Network for Visual Recognition[J]. 2021.
- [8] Xie S, Tu Z. Holistically-nested edge detection[C]//Proceedings of the IEEE international conference on computer vision. 2015: 1395-1403.

- [9] Weng Piao. Research on Pavement Crack Segmentation Algorithm in Complex Environment [D]. Zhengzhou University, 2019.
- [10] Chen L C, Papandreou G, Kokkinos I, et al. DeepLab: Semantic Image Segmentation with Deep Convolutional Nets, Atrous Convolution, and Fully Connected CRFs[J]. IEEE Transactions on Pattern Analysis and Machine Intelligence, 2018, 40(4):834-848.
- [11] Purkait P, Zhao C, Zach C. SPP-Net: Deep Absolute Pose Regression with Synthetic Views[J]. 2017.
- [12] Zhao H, Shi J, Qi X, et al. Pyramid Scene Parsing Network[J]. IEEE Computer Society, 2016.
- [13] Zheng S, Lu J, Zhao H, et al. Rethinking semantic segmentation from a sequence-to-sequence perspective with transformers[C]//Proceedings of the IEEE/CVF Conference on Computer Vision and Pattern Recognition. 2021: 6881-6890.
- [14] Strudel R, Garcia R, Laptev I, et al. Segformer: Transformer for Semantic Segmentation[J]. 2021.
- [15] Ronneberger O, Fischer P, Brox T. U-net: Convolutional networks for biomedical image segmentation[C]//International Conference on Medical image computing and computer assisted intervention. Springer, Cham, 2015: 234-241.
- [16] Chen L C, Zhu Y, Papandreou G, et al. Encoder-Decoder with Atrous Separable Convolution for Semantic Image Segmentation[J]. arXiv, 2018.
- [17] Xie E, Wang W, Yu Z, et al. SegFormer: Simple and Efficient Design for Semantic Segmentation with Transformers[J]. 2021.
- [18] Peng Z, Huang W, Gu S, et al. Conformer: Local Features Coupling Global Representations for Visual Recognition[J]. 2021.
- [19] Dong X, Bao J, Chen D, et al. Cswin transformer: A general vision transformer backbone with cross-shaped windows[J]. arXiv preprint arXiv:2107.00652, 2021.
- [20] Jie, Shen, Samuel, et al. Squeeze-and-Excitation Networks.[J]. IEEE transactions on pattern analysis and machine intelligence, 2019.
- [21] Shi Y, Cui L, Qi Z, et al. Automatic road crack detection using random structured forests[J]. IEEE Transactions on Intelligent Transportation Systems, 2016, 17(12): 3434-3445.
- [22] Zou Q, Cao Y, Li Q, et al. CrackTree: Automatic crack detection from pavement images[J].

Pattern Recognition Letters, 2012, 33(3): 227-238.

- [23] Hu F, Liu J, Yang D, et al. Semantic segmentation of road surface crack images using RU-Net model[C]//Twelfth International Conference on Graphics and Image Processing (ICGIP 2020). International Society for Optics and Photonics, 2021, 11720: 1172014.
- [24] Dong H K, Cha Y J. Efficient attention-based deep encoder and decoder for automatic crack segmentation[J]. 2021. Ju H, Li W, Tighe S, et al. CrackU-net: A novel deep convolutional neural network for pixelwise pavement crack detection[J]. Structural Control and Health Monitoring, 2020(5):e2551.
- [25] Liu H, Miao X, Mertz C, et al. CrackFormer: Transformer Network for Fine-Grained Crack Detection[C]// International Conference on Computer Vision. 2021.